

Modal analysis of the scattering coefficients of an open cavity in a waveguide

Yuhui Tong^a, Jie Pan^{a,*}

^a*School of Mechanical and Chemical Engineering, The University of Western Australia, Crawley, WA 6009, Australia*

Abstract

The characteristics of an acoustic scatterer are often described by scattering coefficients. The understanding of the mechanisms involved in the frequency dependent features of the coefficients has been a challenge task, owing to the complicated coupling between the waves in open space and the modes inside the finite scatterer. In this paper, a frequency-dependent modal description of the scattering coefficient is utilized to study the modal properties of the scatterer. The important role that eigenmodes play in defining the features of the scattering coefficients is revealed via an expansion of the coefficients by the eigenmodes. The results show the local extrema of the scattering coefficients can be attributed to the constructive/destructive interference of resonant and non-resonant modes. In particular, an approximated equation, which is equivalent to the standard Fano formula, is obtained to describe the sharp anti-symmetric Fano characteristics of the scattering coefficients. The special cases where scattering is dominated by a single resonance eigenmode, corresponding to the “resonance transmission”, are also illustrated.

Keywords: Open cavity; Scattering coefficient; Eigenmode; Fano resonance

1. Introduction

The scattering coefficients of acoustic scatterers are important parameters as they are used to relate incident and scattered waves. Traditionally, sound scattering in a duct by a muffler is described by one-dimensional

*Corresponding author

Email address: jie.pan@uwa.edu.au (Jie Pan)

Preprint submitted to *Wave Motion*

June 21, 2016

(1D) transmission line theory, and explained by the mismatch of the specific impedance at the inlet and outlet of the muffler [1]. To accommodate cross modes in a duct with scatterers, the wave matching technique [2, 3] is used. The finite element and boundary element methods, are used to determine the scattering coefficients when the geometries of the ducts and scatterers are complicated [4, 5]. While these wave matching and numerical methods are capable of producing accurate coefficients, they are less useful in directly delivering the physical insight into the peaks and valleys in the coefficient curves.

An alternative approach, which is motivated by the observation of trapped and quasi-normal modes inside the scatterers, is to describe the scattering in terms of the coupling between the waves in the ducts and modes inside the scatterer. This was inspired by the early work of Flax *et al.* [6], where the sound scattering from submerged elastic bodies is affected by various kinds of interference between the resonance scattering at the eigenfrequencies of the vibration of the body and the rigid-body scattering. Recently, such approach has been used to explain the peaks and valleys in the transmission loss curve of an expansion chamber subject to an incident plane-wave in a 1D duct [7]. It was demonstrated that the characteristics (complex eigenvalues and mode shape functions) of the frequency-dependent quasi-normal modes of the expansion chamber [8] allow the correct expansion of the sound pressure in the chamber. The coupling of the quasi-normal modes with the incident and transmitted sound waves sheds some light on the transmission loss. For example, the minimum values in the transmission loss occur when the frequency of the incident wave equals the real part of the eigenfrequency of the quasi-normal mode. On the other hand, the maximum transmission loss appears at those frequencies where the superimposed contribution from the participated modal factors is at minimum. However, the extension of these previous works to two-dimensional (2D) or three-dimensional (3D) expansion chambers and modelling of the coupling between the quasi-modes in the chambers and the incident and transmitted waves including cross modes, is not straight forward. Furthermore, because of the involvement of cross mode components in the 2D and 3D configurations, extra coupling mechanisms due to participation of the cross modes may lead to a more complete understanding of the characteristics of the scattering coefficients.

Most recently, Maksimov *et al.* [9] and Lyapina *et al.* [10] looked at the aforementioned scattering problem from a more fundamental view of the

acoustical properties of an open cavity. An open cavity is a finite acoustical space with defined boundary conditions at its internal wall (*e.g.*, a rigid-wall condition) and some boundary areas open to infinite space(s), such as semi-infinite waveguides. Because of the energy exchange between the sound fields inside the open-cavity and the infinite space(s), the sound field inside the cavity is characterized by the non-Hermitian Hamiltonian. They used the acoustic coupled mode theory for the calculation of the frequency-independent eigensolutions of the open cavity and revealed a mechanism resulting in acoustic trapped modes in the cavity, namely Friedrich–Wintgen two-mode full destructive interference. Although being used to explain the occurrence of Fano resonance, the nonorthogonal properties and incompleteness of the frequency-independent eigensolutions of the open cavity make the direct modal interpretation of the transmission coefficient (which is a forced scattering problem at the frequency of an incident wave) a difficult task. Xiong *et al.* [11], on the other hand, derived the scattering matrix of the open cavities due to incident waves from one of the waveguide connected to the cavity. Frequency-dependent eigensolutions of the effective Hamiltonian matrix (including the interaction between cavity and connected waveguides) for the sound field in the cavity were used to describe the scattering coefficients and to explain the links between the eigenmodes and a trapped mode and the corresponding transmission zero. Their contribution makes possible an analysis of the scattering coefficients of the open cavities by using the frequency-dependent eigensolutions of the cavity.

In this paper, the method for frequency-dependent eigenmodes and the scattering matrix developed by Xiong *et al.* [11] is adopted. Instead of focusing on the Fano resonance induced by trapped modes, it is used to calculate and explain the general scattering features of the open cavities connected with waveguides (*e.g.*, conventional muffler configuration) and the roles played by eigenmodes in determining the frequency-dependent features of the scattering coefficients. Through numerical studies, it is revealed that extrema in scattering coefficients are *generally* a result of interference between eigenmodes, rather than the contribution from single resonant mode, as is traditionally assumed. The Fano resonance induced by highly localized modes (quasi-trapped modes), as observed by Hein *et al.* [12], is also revisited in terms of frequency-dependent eigenmodes. Finally, some remarks are made to clarify the usage of frequency-dependent and frequency-independent modes in conducting modal analysis in scattering problems.

2. Modal description of the scattering coefficients

This paper considers the scattering problem in a 2D acoustic scatterer, comprising a cavity connected by N uniform ducts. Omitting the time-dependence term, $e^{-i\omega t}$, the sound pressure field is governed by Helmholtz equation.

$$(\frac{\partial^2}{\partial x^2} + \frac{\partial^2}{\partial y^2} + k^2)p(x, y) = 0, \quad (1)$$

and corresponding boundary conditions, where k is the wavenumber. Since $k = \omega/c_0$ (where c_0 is the speed of sound), k will be used hereafter to represent source frequency, *i.e.*, whenever “frequency” is mentioned, it refers to the wavenumber. For the sake of simplicity, the rigid-wall boundary condition is assumed for the cavity and ducts. Although details of the coupled mode theory [9, 10, 11] have already been published, this paper provides a brief description of the derivation using coupled mode theory for the scattering coefficients of the scatterer in terms of frequency-dependent eigenmodes, for the convenience of the reader and to make the paper self-contained.

The first step is to express the sound pressure in terms of a local basis in different regions. The geometry is partitioned into $(N+1)$ regions: a closed cavity Ω_c and N semi-infinite ducts Ω_n ($n = 1, 2, \dots, N$). The pressure field in the n^{th} duct is expanded into duct modes when taking a local coordinate (x_n, y_n) with x - and y -axes that are, respectively, perpendicular and vertical to the n^{th} duct-cavity interface:

$$p(x_n, y_n) = \sum_p (a_{n,p} e^{-i\kappa_{n,p} x_n} + b_{n,p} e^{-i\kappa_{n,p} x_n}) \chi_{n,p}(y_n), \quad (2)$$

where $a_{n,p}$ and $b_{n,p}$ are respectively, the amplitude for the p^{th} *incident* and *scattered* modes. The transverse functions $\chi_{n,p}(y)$ are given by $\chi_{n,p}(y_n) = \sqrt{\frac{2-\delta_{0,p}}{d_n}} \cos(\frac{p\pi}{d_n} y_n)$, where d_n is the width of the n^{th} duct. Finally, $\kappa_{n,p}$ is the axial wavenumber such that, $\kappa_{n,p} = \sqrt{k^2 - (p\pi/d_n)^2}$, ($p = 0, 1, 2, \dots$)

The pressure field in the cavity may be expanded by closed cavity modes such that

$$p(x, y) = \sum_{\mu} g_{\mu} \psi_{\mu}(x, y). \quad (3)$$

where $\psi_{\mu}(x, y)$ is the *closed* cavity mode satisfying

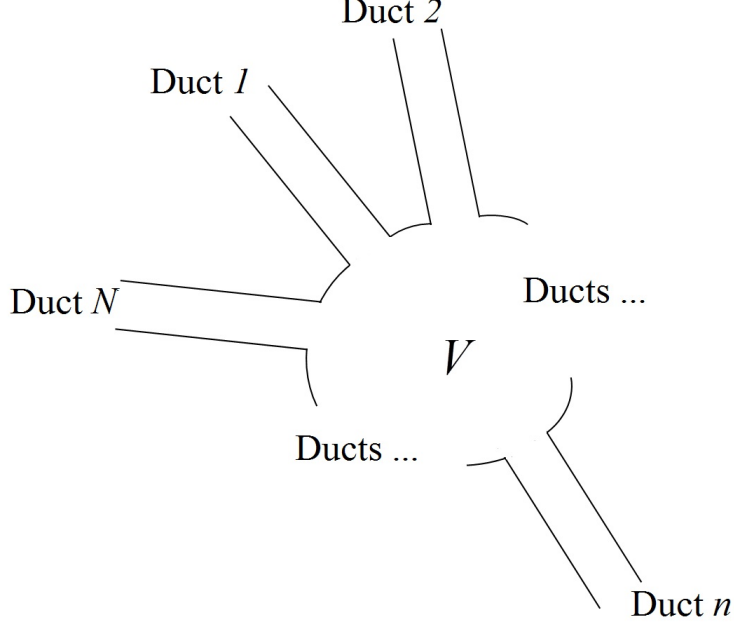


Figure 1: An open cavity connected with N uniform rigid-wall ducts.

$$\left(\frac{\partial^2}{\partial x^2} + \frac{\partial^2}{\partial y^2} + k_\mu^2\right)\psi_\mu(x, y) = 0, \quad (4)$$

with Numann (rigid) boundary conditions at the duct-cavity interfaces and at other boundary surface of the cavity, where k_μ is the eigenvalue.

Although $\psi_\mu(x, y)$ does not satisfy the continuity condition for particle velocity at the cavity-duct interfaces, it is worth emphasizing that the expansion in Eq. (3) is valid as the matching conditions for particle velocity must not be imposed directly, which is a consequence of the fact that the convergence in Hilbert space does not imply point-wise convergence at the boundary [13, 14].

In a third step, a key equation is derived to determine the coefficient g_μ for the cavity upon incident waves by applying the continuity condition of pressure and velocity in a limiting sense infinitesimally close to the boundary:

$$\left(\mathbf{D} - k^2 \mathbf{I}\right) \mathbf{g} = -2i \sum_{n=1}^N \sum_{p=1}^{+\infty} \kappa_{n,p} \mathbf{v}_{n,p} a_{n,p}, \quad (5)$$

where \mathbf{I} is the identity matrix, \mathbf{g} is an unknown column vector containing the coefficients g_μ . The column vector $\mathbf{v}_{n,p}$ contains the coupling constant $v_{n,p}^\mu$ between the rigid cavity mode ψ_μ and the duct mode $\chi_{n,p}$ [9, 15], *i.e.*, $v_{n,p}^\mu = \int \psi_\mu \chi_{n,p} d\tau_n$, where the integral is evaluated over the interfaces between the cavity and the n^{th} duct, and τ_n is the corresponding surface element. The matrix \mathbf{D} has the following form:

$$\mathbf{D} = \mathbf{k}_c^2 - i \sum_{n=1}^N \sum_{p=1}^{+\infty} \kappa_{n,p} \mathbf{v}_{n,p} \mathbf{v}_{n,p}^\dagger, \quad (6)$$

where \mathbf{k}_c^2 is a diagonal matrix containing the squared eigenfrequencies k_μ^2 , and symbol \dagger denotes the conjugate transpose. It then follows that the scattered wave $b_{n,p}$ (the p^{th} outgoing duct mode in the n^{th} duct) is found as

$$b_{n,p} = -a_{n,p} + \mathbf{v}_{n,p}^\dagger \mathbf{g}. \quad (7)$$

The scattering coefficients $s_{n,n',p,p'}$ are defined by $b_{n,p} = \sum_{n',p'} s_{n,n',p,p'} a_{n',p'}$. Substituting the solution of Eq. (5) into Eq. (7) yields

$$s_{n,n',p,p'}(k) = -\delta_{n,n'} \delta_{p,p'} - 2i \mathbf{v}_{n,p}^\dagger \frac{1}{(\mathbf{D} - k^2 \mathbf{I})} \kappa_{n',p'} \mathbf{v}_{n',p'}, \quad (8)$$

which relates the scattered wave $b_{n,p}$ to the incident wave $a_{n',p'}$.

In a fourth step, an eigenvalue problem (EVP) of \mathbf{D} subject to the source frequency k is solved as

$$\mathbf{D}(k) \mathbf{G}_\mu = K_\mu^2 \mathbf{G}_\mu, \quad (9)$$

where K_μ^2 and \mathbf{G}_μ are respectively the frequency-dependent eigenvalue and eigenvector. Since $\mathbf{D}(k)$ is a non-Hermitian matrix, its eigenvectors satisfy the bi-orthogonal relation (see Appendix),

$$\mathbf{G}_{\mu'}^T \mathbf{G}_\mu = \delta_{\mu',\mu}, \quad (10)$$

where the superscript T denotes a transpose. Alternatively, Eq. (10) may be written as

$$\iint_{\Omega_c} \Psi_{\mu'}(x, y) \Psi_\mu(x, y) ds_c = \delta_{\mu,\mu'}, \quad (11)$$

where $\Psi_\mu(x, y)$ is the mode-shape function corresponding to \mathbf{G}_μ . Note that

the integral is evaluated over Ω_c , the domain occupied by the cavity,.

Finally, expanding \mathbf{g} in Eq. (5) in terms of eigenvectors of $\mathbf{D}(k)$, *i.e.*, $\mathbf{g} = \sum_{\mu} c_{\mu} \mathbf{G}_{\mu}$, and substituting it into Eq. (7) yields the expression for scattering coefficients in terms of eigenmodes

$$s_{n,n',p,p'} = -\delta_{n,n'}\delta_{p,p'} + \sum_{\mu} \frac{-2i\kappa_{n',p'} H_{\mu,n',p'} H_{n,p,\mu}}{K_{\mu}^2 - k^2}, \quad (12)$$

where $H_{\mu,n',p'} = \mathbf{G}_{\mu}^T \mathbf{v}_{n',p'}$ and $H_{n,p,\mu} = \mathbf{v}_{n,p}^{\dagger} \mathbf{G}_{\mu}$.

Compared with Eq. (8), Eq. (12) expresses the scattering coefficients explicitly as a superposition of individual eigenmode components. The first term on the right-hand side of Eq. (12) comes from the direct reflection, while each term in the summation corresponds to scattering by eigenmode \mathbf{G}_{μ} . The term $H_{\mu,n',p'}$ measures the coupling between eigenmode \mathbf{G}_{μ} and the incident duct mode (n', p') . Similarly, $H_{n,p,\mu}$ provides a measurement of the coupling between eigenmode \mathbf{G}_{μ} and the scattered duct mode (n, p) .

3. Results and discussions

The aim of this section is to demonstrate the role that the eigenmodes of the acoustic scatterer play in sound scattering, which is a question originally put forward by [16] in their analysis of wave propagation in continuous right-angled bends. This question can now be answered mathematically using Eq. (12), by showing that scattering coefficients can indeed be expressed in terms of the eigenmodes of an acoustic scatterer. Numerical results will be used to support this answer.

In Eq. (12), the summation terms are characterized by the inverse of $(K_{\mu}^2 - k^2)$. One might therefore assume that $s_{n,n',p,p'}$ is dominated by each eigenmodes within each frequency range and that $|s_{n,n',p,p'}|$ achieves extreme values. The numerical study, however, will show that the local extrema of the scattering coefficients, are generally the result of constructive or destructive interference of eigenmodes, rather than by dominating resonance alone as one would expect intuitively. In the following parts of this section, the typical interference of eigenmodes will be covered first in Sec. 3.1. Then Sec. 3.2 will discuss a special narrow band interference known as Fano Resonance. Section 3.3 will be devoted to the phenomenon of resonance transmission.

It is worth noting that, although the theory proposed in Sec. 2 is valid for scatterers of arbitrary-shape and with multiple connecting ducts, for

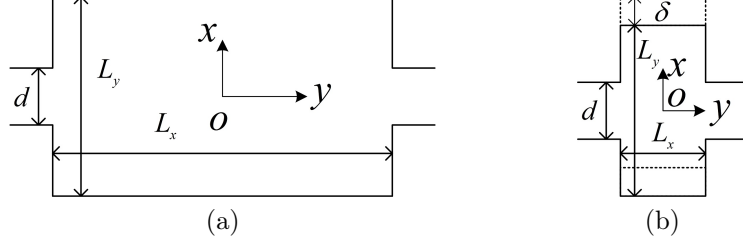


Figure 2: Geometries of (a) long cavity (b) short cavity.

the sake of simplicity, the numerical study will be restricted to scatterers consisting a rectangular cavity connected by two uniform ducts, with the geometries illustrated in Fig. 2. The scatterer with two connecting ducts is the simplest yet sufficiently representative of its kind, whereas a rectangular cavity enables an analytical solution of the closed cavity modes $\psi_\mu(x, y)$; otherwise, the complexity of mode classification and subsequent analysis may mask important physical phenomena.

In the following context, symbols L and R are used to denote ducts on the left- and right-hand sides, respectively. The scattering coefficients, owing to the symmetry of the systems, are reduced to the transmission and reflection coefficients, $T_{p,p'}$ and $R_{p,p'}$, respectively. For simplicity, only $T_{p,p'}$ is examined here. Using Eq. (12) and modal decomposition by each eigenmode μ , $T_{p,p'}$ is expressed as

$$T_{p,p'} = \sum_{\mu} T_{p,p',\mu}, \quad (13)$$

where

$$T_{p,p',\mu} = \frac{-2i\kappa_{n',p'} H_{\mu,n',p'} H_{n,p,\mu}}{K_{\mu}^2 - k^2}. \quad (14)$$

and μ is the index of the μ^{th} bi-orthogonal eigenmodes. For a rectangular cavity where variable separation is possible, μ is represented by a pair of non-negative values (m, n) . The analysis of $R_{p,p'}$ is omitted as it can be conducted following the same procedures.

3.1. Typical case: interference of eigenmodes

The first to be considered is a short expansion cavity, depicted by Fig. 2(b), which supports a typical case of interference for eigenmodes. The system parameters are $d = 1$ m, $L_x = 1$ m and $L_y = 3$ m, and an ad-

justable vertical offset δ is used to dictate the geometrical symmetry about the x -axis ($\delta = 0$ is considered here). Since the length of the cavity, L_y , is comparable with its width, L_x , one can anticipate that the 2D modes with non-uniform transverse functions may play an important role in sound scattering.

Figure 3(a) presents the amplitude of $|T_{0,0}|$ versus frequency. Several peaks are observed at $k = 0 \text{ m}^{-1}$ and $k = 2.94 \text{ m}^{-1}$ and several dips at $k = 1.68 \text{ m}^{-1}$ and $k = 3.42 \text{ m}^{-1}$. Using Eq. (13), one can decompose $|T_{0,0}|$ into a contribution by individual eigenmodes. Due to the transversal symmetry of the system, only transversally symmetric modes can participate in the scattering of the plane wave, *i.e.*, only the $(0,0)$, $(0,2)$ and $(1,0)$ modes need to be taken into account for $k < 3.5 \text{ m}^{-1}$. Figure. 3(d) and (e) show K_μ , which are the eigenvalues of the corresponding modes. It is noted that $Re(K_\mu)$ ($\mu = (0,0)$, $(0,2)$ and $(1,0)$) varies slowly with k except for $Re(K_{(0,0)})$, while $Im(K_\mu)$ always start from 0 when $k = 0 \text{ m}^{-1}$ and decreases rapidly as k increases. Figure 3(d) shows the components of $T_{0,0}$, *i.e.*, $T_{0,0,\mu}$ ($\mu = (0,0)$, $(0,2)$, $(1,0)$), as functions of k . When k approaches $Re(K_\mu)$, the modal transmission coefficient of the μ^{th} mode experiences resonance, leading to the resonance peak of each $|T_{0,0,\mu}|$, *e.g.*, at $k = 0 \text{ m}^{-1}$ for $\mu = (0,0)$, at $k = 2.18 \text{ m}^{-1}$ for $\mu = (0,2)$ and at $k = 3.42 \text{ m}^{-1}$ for $\mu = (1,0)$. The width of each resonance peak, on the other hand, is dictated by $Im(K_\mu)$, *e.g.*, $|T_{0,0,(0,2)}|$ has a wide peak as $Im(K_{(0,2)})$ grows large, while the peak of $|T_{0,0,(1,0)}|$ is relatively narrow as $Im(K_{(1,0)})$ grows small.

A comparison between Fig 3(a) and Fig. 3(b) indicates that there are no direct relations between the peaks of $|T_{0,0,\mu}|$ and the extrema of $|T_{0,0}|$ (except for the first peak at $k = 0 \text{ m}^{-1}$, which will be discussed in Sec. 3.3). Instead, the local minimum in $|T_{0,0}|$ at $k = 1.68 \text{ m}^{-1}$ is due to the destructive interference between the $(0,2)$, $(0,0)$ and $(1,0)$ modes. The local maximum at $k = 2.9 \text{ m}^{-1}$ arises from the constructive interference between $(0,2)$, $(1,0)$, and $(0,0)$ eigenmodes, whereas the destructive interference between $(0,2)$ and $(1,0)$ gives rise to the local minimum of $|T_{0,0}|$ at $k = 3.42 \text{ m}^{-1}$.

Figure 4(a) depicts the amplitude of the transmission coefficient of the 0^{th} waveguide mode, $T_{0,0}$, for a long cavity ($d = 1 \text{ m}$, $L_x = 5 \text{ m}$ and $L_y = 2 \text{ m}$), as shown in Fig. 2(a). Within the frequency range of interest ($k < 3.5 \text{ m}^{-1}$), the components of $T_{0,0}$, *i.e.*, $|T_{0,0,\mu}|$ are mainly due to the first five eigen-modes ($\mu = (0,0)$, $(1,0)$, $(2,0)$, $(3,0)$, $(4,0)$) of the open cavity. Figure 4(b) shows that $|T_{0,0,\mu}|$ are also characterized by their resonance peaks. The comparison between Fig. 3(d) and Fig. 4(g) suggests that the local extrema

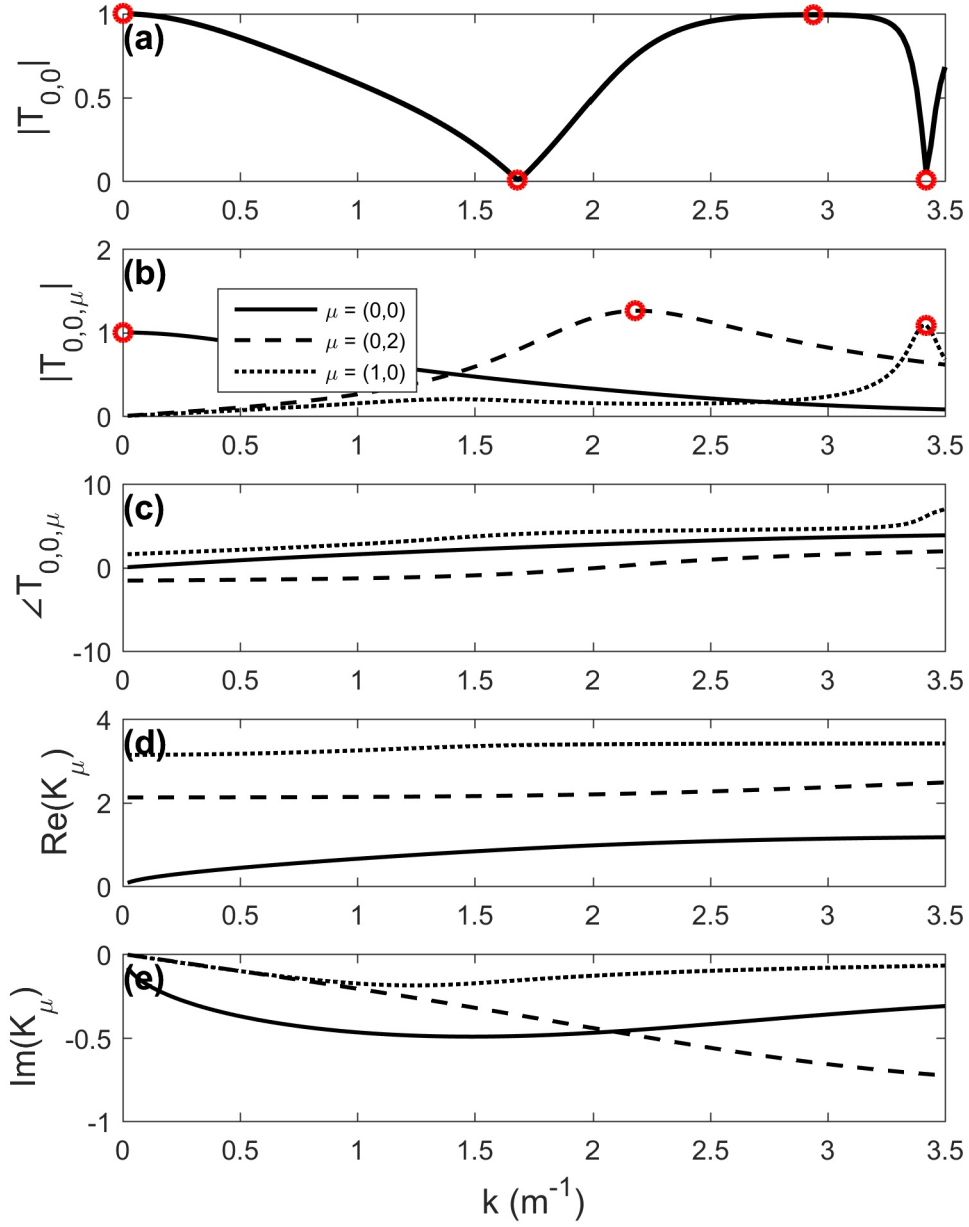


Figure 3: The spectra and physical quantities related to the transmission coefficient $T_{0,0}$ for a transversally symmetric short cavity: (a) the amplitude of transmission coefficient $T_{0,0}$, (b) and (c) the amplitude and phase (rad) of a component of $T_{0,0}$, *i.e.*, $T_{0,0,\mu}$ versus k , (d) and (e) the real and imaginary parts of eigenvalue K_μ versus k .

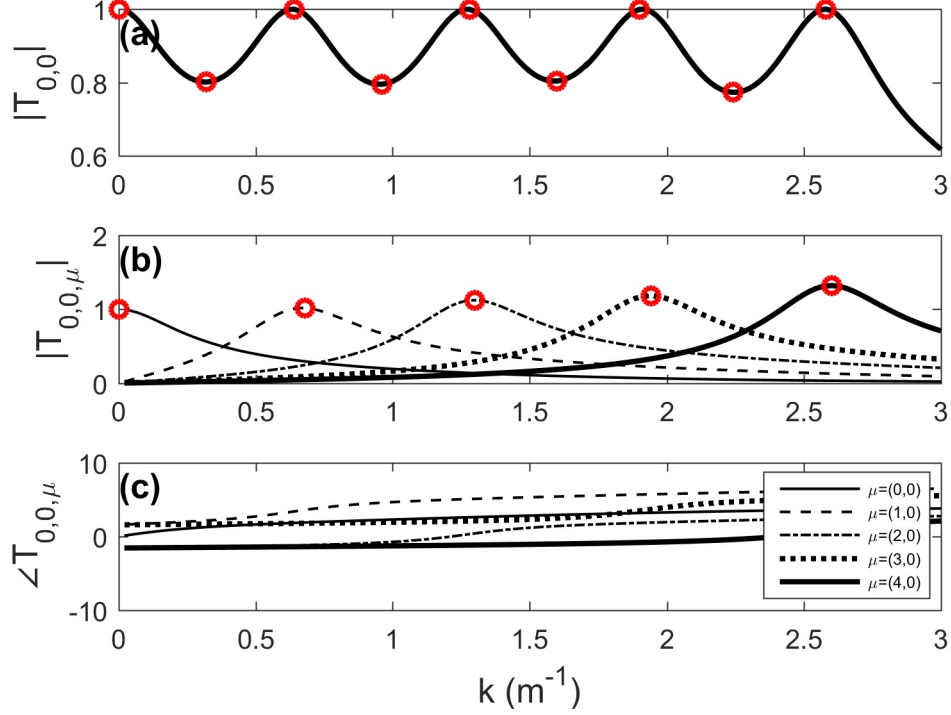


Figure 4: The spectra and physical quantities related to the transmission coefficient $T_{0,0}$ for a long chamber: (a) the amplitude of transmission coefficient $T_{0,0}$, (b) and (c) the amplitude and phase (rad) of five components of $T_{0,0}$.

in $|T_{0,0}|$ of the long cavity are also due to the superposition of eigenmodes. For example, at $k = 0.68 \text{ m}^{-1}$, the maximum of $|T_{0,0}|$ is not caused by the resonance peak of $|T_{0,0,(1,0)}|$ alone, while $|T_{0,0,(0,0)}|$ and $|T_{0,0,(2,0)}|$ also have non-negligible contributions to the transmission coefficient. However, the latter two terms cancelled each other leaving the (1,0) eigenmode of the cavity as the sole contributor to $T_{0,0}$ at frequencies around $k = 0.68 \text{ m}^{-1}$. A similar analysis can be made for the other $|T_{0,0}|$ peaks, except for the first one at $k = 0 \text{ m}^{-1}$, which is a case of resonance transmission (to be discussed in Sec. 3.3). The dips in $|T_{0,0}|$, on the other hand, are due to the destructive interference of the eigenmodes.

3.2. Fano resonance

The eigenmodes responsible for the transmission coefficients in Figs. 3 and 4 have relatively large imaginary parts. The open cavity also has another type of eigenmodes, known as quasi-trapped modes, whose eigenvalues have very small imaginary part and hence result in very narrow resonance peaks. Although the involvement of quasi-trapped modes in producing the sharp asymmetric Fano resonance is well known [17, 12, 11], the theoretical analysis in Sec. 2. will be used to explain how these quasi-trapped modes are involved in producing the Fano resonances.

Consider again the short cavity with parameters of $d = 1$ m, $L_x = 1$ m, $L_y = 3$ m, and $\delta = 0.1$ m. For this case the quasi-trapped modes emerge as an offset is introduced to make the cavity asymmetric about the central axis [12]. Figure 5(a) presents the amplitude of $|T_{0,0}|$ versus k . Compared with Fig. 3(a), it is found that extra peaks and dips emerge around $k = 1.15 \text{ m}^{-1}$ and $k = 3.14 \text{ m}^{-1}$ in Fig 5(a), showing typical Fano resonances. To explain the formation of the Fano resonances, the contribution to $T_{0,0}$ of each individual mode is plotted in Fig. 5(b). Due to the broken transversal symmetry, the original fully localized modes (0,1) and (0,3) modes become quasi trapped modes with $\text{Re}(K_{(0,1)}) \sim 1.15 \text{ m}^{-1}$ and $\text{Re}(K_{(0,3)}) \sim 3.14 \text{ m}^{-1}$, now participate in the coupling with the waveguide waves. As shown in Figs 5(b) and (c), that $K_{(0,1)}$ and $K_{(0,3)}$ now have very small imaginary parts. In Fig. 5(b), $|T_{0,0,(0,1)}|$ and $|T_{0,0,(0,3)}|$ display sharp resonance behaviors; the corresponding sharp phase changes are also observed in Fig. 5(c) at the peak frequencies.

An interpretation of this phenomenon is straightforward following the wave superposition expression in Eq. (12). Taking the first Fano resonance ($k \approx 1.15 \text{ m}^{-1}$) as an example, in the vicinity of $k = 1.15 \text{ m}^{-1}$, the quasi-trapped mode (0,1) demonstrates a resonance response, and hence $T_{0,0,(0,1)}$ has a sharp phase change, while the responses of the other modes vary slowly in terms of amplitude and phase. Therefore, below and above the resonance frequency of $T_{0,0,(0,1)}$, constructive and destructive interferences between $T_{0,0,(0,1)}$ and components of other eigenmodes give rise to a local maximum and minimum, respectively, of the $T_{0,0}$. The contribution by non-resonance modes can be approximated by a complex constant. As a result, the Fano resonance can be characterized as the superposition of a resonantly excited eigenmode μ (here, $\mu = (0,1)$) and background non-resonance response c_1 , *i.e.*,

$$\begin{aligned}
T_{0,0} &= T_{0,0,\mu} + \sum_{\mu' \neq \mu} T_{0,0,\mu'} \\
&\approx T_{0,0,\mu} + c_1 \\
&\approx \frac{c_2}{\mathcal{K}_\mu^2 - k^2} + c_1
\end{aligned} \tag{15}$$

where in the third row, the numerator of the first term, originally expressed as $\kappa_{R,0} H_{\mu,\nu,L,0} H_{R,0,\mu,\nu}$ in Eq. (12), is approximated by a constant c_2 , and K_μ in the denominator by a constant \mathcal{K}_μ . The approximations are valid for the narrow bandwidth in which Fano resonance occurs, as the approximated terms vary slowly with frequency. The frequency-dependent K_μ can be taken as a constant \mathcal{K}_μ , as K_μ is almost a constant within the frequency band.

On the other hand, it is well known that the standard Fano formula [18] in terms of sound power transmission, in *the vicinity* of $Re(K_{(0,1)})$ can be written as:

$$T_{standard}(k) = \sigma \left(q + \frac{k - Re(\mathcal{K}_{(0,1)})}{Im(\mathcal{K}_{(0,1)})} \right)^2 / \left[1 + \left(\frac{k - Re(\mathcal{K}_{(0,1)})}{Im(\mathcal{K}_{(0,1)})} \right)^2 \right], \tag{16}$$

where $(k - Re(\mathcal{K}_{(0,1)}))/Im(\mathcal{K}_{(0,1)})$ is the reduced resonance frequency, q measures the asymmetry of the resonance shape, and σ is the normalization constant.

A way to verify Eq. (15) is to fit the $T_{0,0}(k)$ to the actual sound power transmission curve to determine the value of \mathcal{K}_μ and check if it agrees with K_μ by eigensolution (Eq. (9)) within the narrow band. It is shown in Fig. 6 the original and fitted curve of $T(k) = |T_{0,0}|^2$ using Eq. (15) in Fig. 6., Excellent agreement is observed between the actual sound power transmission curve and the fitted curve using Eq. (15), while the fitted parameter $\mathcal{K}_{(0,1)}$ is also very close to the frequency-dependent eigen-value $K_{(0,1)}$ at the resonance frequency for $k = 1.145 \text{ m}^{-1}$ of the (0,1) eigenmode, as is shown in Table. 1. The results of curve fitting indicate that Eq. (15) indeed serves as a good description of the Fano resonance caused by the quasi trapped mode (0,1).

A further observation, according to Fig. (6) and Table. 1, is that the fitted curve using Eq. (15) agrees well with that using the standard Fano

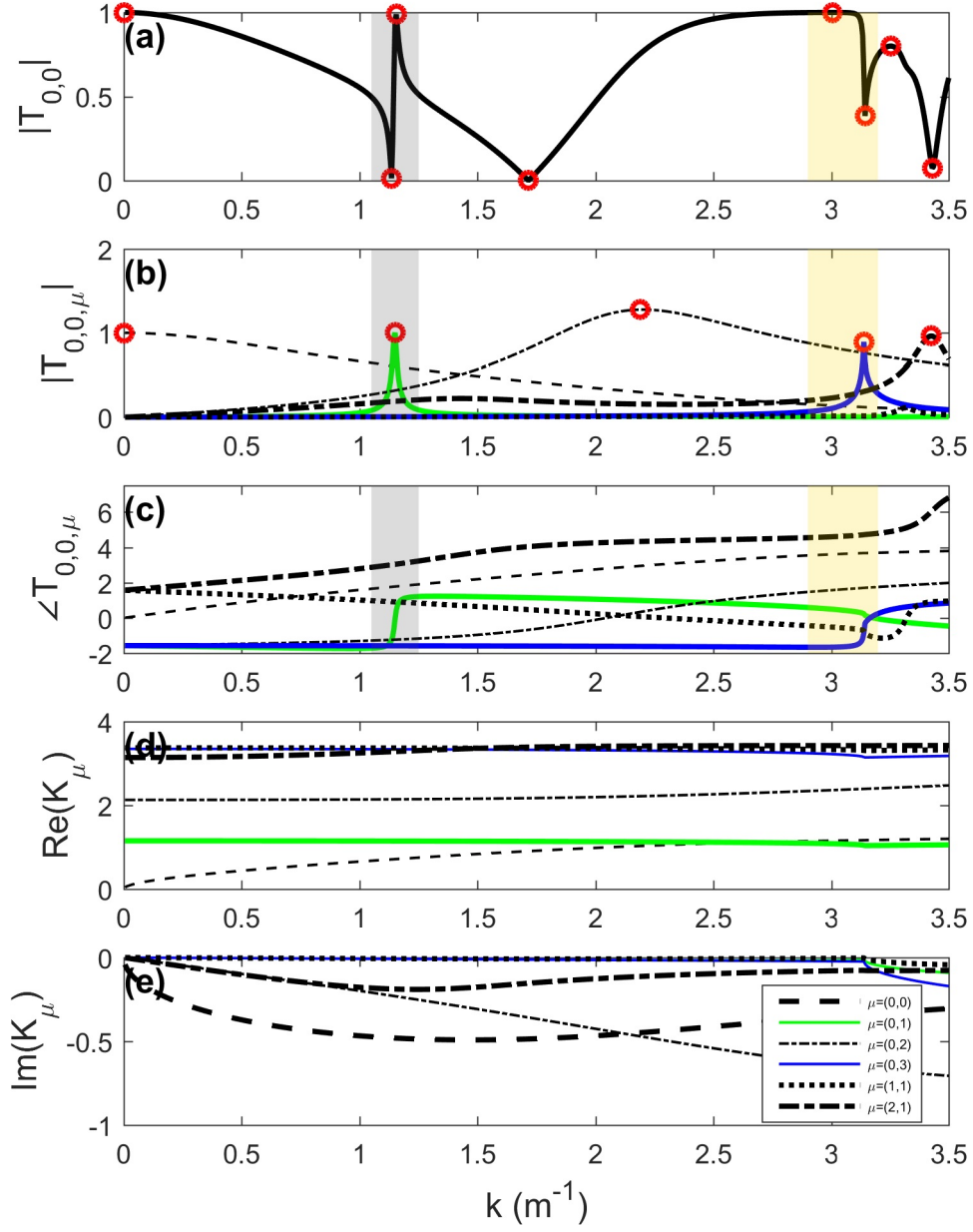


Figure 5: Spectra and physical quantities related to transmission coefficient $T_{0,0}$ for a transversally asymmetric short duct: (a) The amplitude of $T_{0,0}$, (b) and (c) the amplitude and phase (rad) of $T_{0,0,\mu}$, and (d) and (e) the real and imaginary parts of K_μ .

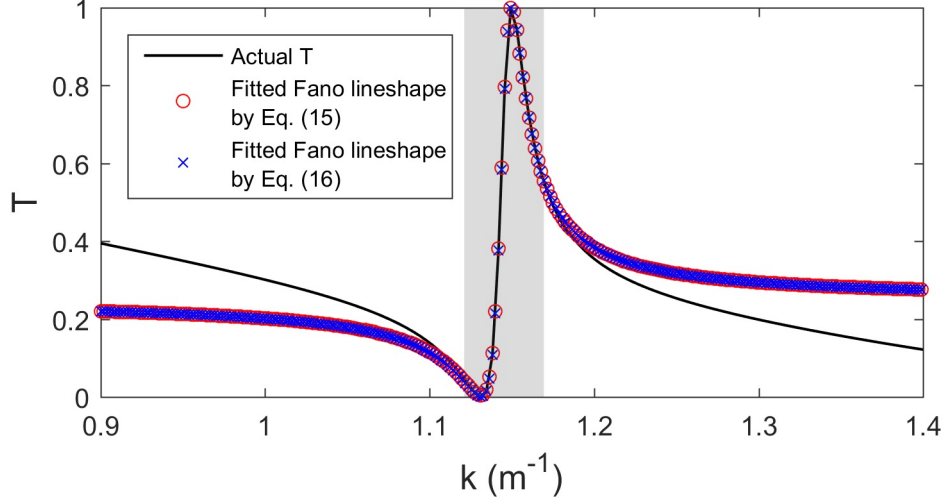


Figure 6: The sound power transmission coefficient T : (solid line) actual $T(k)$ calculated using Eq. (13), (circles) fitted curve using Eq. (15) and (crosses) fitted curve using Eq. (16).

formula in Eq. (16). It is interesting that the two fitted curves exhibit excellent agreement not only within the narrow band where Fano resonance occurs, but at other frequencies as well. It is an indicator that Eq. (15) is actually equivalent to the standard Fano formula - they cannot agree globally unless they are describing the same function of k , or more explicitly, they agree globally because they are equivalent and are describing the same function of k .

Methods	$Re(K_{(0,1)})$ or $Re(\mathcal{K}_{(0,1)})$	$Im(K_{(0,1)})$ or $Im(\mathcal{K}_{(0,1)})$	Parameters
EVP ($k = 1.145 \text{ m}^{-1}$)	1.146	-0.0848	
Curve fitting I	1.145	-0.0836	$ c_2 = 0.0174,$ $c_1/c_2 = -26.31 + 11.73i$
Curve fitting II	1.145	-0.0839	$q = 1.744, \sigma = 0.2478$

Table 1: Eigenvalues obtained by (1) solving the EVP directly and (2) and (3) curve fitting using Eq. (15) and (16), respectively.

3.3. Resonance transmission

The first local maximum in $|T_{0,0}|$ in Figs. 3(a), 4(a) and 5(a), at $k = 0 \text{ m}^{-1}$, is contributed by the resonance peak of $|T_{0,0,(0,0)}|$ only, while the components of all other eigenmodes are negligibly small. In other words, the transmission peak at $k = 0 \text{ m}^{-1}$ in $|T_{0,0}|$ is dictated by the resonance of (0,0) mode alone, and hence is called “resonance transmission” to distinguish it from the cases discussed in Sec. 3.1 and 3.2, where destructive and constructive superposition of eigenmodes led to local extrema in the scattering coefficients. The condition for the occurrence of resonance transmission is very strict in that it requires the scattering to be dominated by individual modes. In some cases, these conditions are fulfilled such that resonance transmission can be observed. It is considered the scattering coefficient $T_{1,0}$ for the same asymmetrical short cavity discussed in Sec 3.2. Figures 7(a) and (b) present respectively the amplitude of $T_{1,0}$ and the modal components $T_{1,0,\mu}$, and the comparison of these indicates resonance transmission at $k = 1.15 \text{ m}^{-1}$ and $k = 3.14 \text{ m}^{-1}$.

At the first resonance transmission ($k = 1.15 \text{ m}^{-1}$), $T_{1,0}$ is almost dominated by $T_{1,0,(0,1)}$, the modal component by (0,1) eigen-mode. Figures. 7(d) and (e) demonstrate that the modal coupling factors $H_{\mu,L,0}$ and $H_{R,1,\mu}$ exert a crucial influence, as generally only when both of them take relatively large values can $T_{1,0,\mu}$ play an important role in $T_{1,0}$. For example, $T_{1,0,(0,0)}$ corresponds to a small $|H_{R,1,(0,0)}|$ and a large $|H_{(0,0),L,0}|$, leading to an ignorable transmitted wave $b_{R,1}$ owing to the poor coupling between the (0,0) eigenmodes and the transmitted first order duct modes, despite the fact that the (0,0) eigenmode is sufficiently excited by the incident plane wave $a_{L,0}$. A similar reasoning applies to $T_{1,0,(0,2)}$, where the (0,2) eigenmode has a negligible contribution to $T_{1,0}$ owing to the small $|H_{R,1,(0,2)}|$, *i.e.*, the poor coupling between the (0,2) modes and the transmitted first order duct mode.

The above observation, however, does not hold for the squasi trapped mode (0,1). Although $|H_{(0,1),L,0}|$ is small (owing to weak coupling between the (0,1) eigenmode and the incident plane wave $a_{L,0}$), the component of $T_{1,0}$ from the (0,1) mode is still large. It is reasoned that the eigenvalue $K_{(0,1)}$ of the quasi trapped mode (0,1) is almost real, giving $1/(K_{(0,1)}^2 - k^2)$ in Eq. (14), and hence the $T_{1,0,(0,1)}$ term very large value when k is close to $\text{Re}(K_{(0,1)})$. Therefore, in such a situation, only the (0,1) eigenmodes contributes significantly to the $T_{1,0}$ at $k = 1.15 \text{ m}^{-1}$, where $|T_{1,0}|$ achieves its local maxima. In the same way, it is possible to show that the resonance

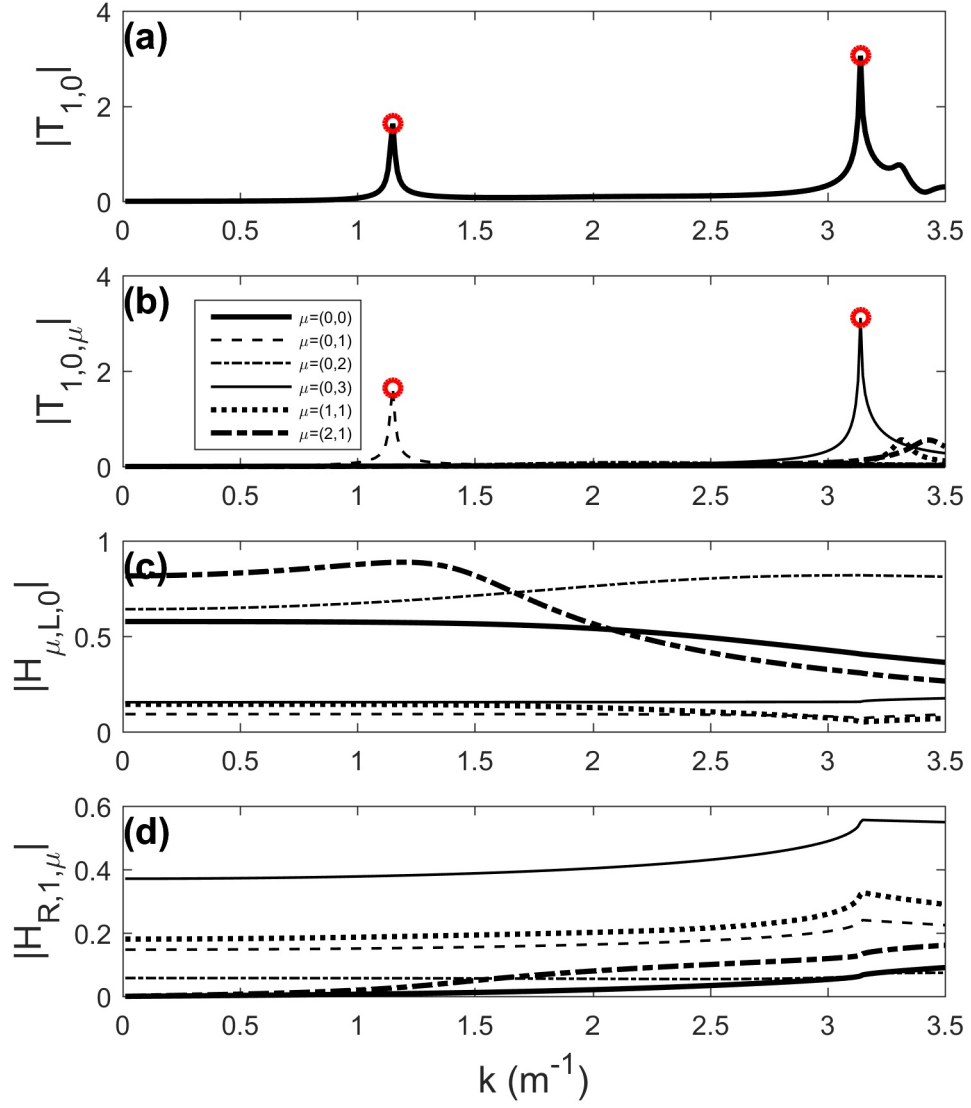


Figure 7: The amplitude of (a) $T_{1,0}$, (b) $T_{1,0,\mu}$, (c) $H_{\mu,L,0}$, and (d) $H_{R,1,\mu}$, for a short cavity.

transmission close to $k = 3.14 \text{ m}^{-1}$ is dominated by (0,3) mode.

It is noted that, in Fig. 7(a) $|T_{1,0}|$ is sometimes greater than 1. For the peak around $k = 1.15 \text{ m}^{-1}$, $|T_{1,0}|$ takes a value of around 1.8, however, it does not correspond to any transmitted sound power as the first-order mode is evanescent and carrying zero net energy flux when $k < \pi \text{ m}^{-1}$. At frequencies around $k = 3.14 \text{ m}^{-1}$, the axial wavenumber is very small, meaning that the transmitted sound power carried by the first order duct mode is actually less than that carried by the incident zeroth-order duct mode, even when $|T_{1,0}|$ is greater than unity.

4. Further discussion about Eq. (9)

In Eq. (12), the bi-orthogonal eigenmodes defined by Eq. (9) are used to decompose the scattering coefficients, and have been employed throughout this paper. They are *frequency-dependent*. It is noted that Eq. (8) can also be used to define another type of EVP, which gives rise to the *frequency-independent* eigenmodes, satisfying,:

$$\mathbf{D}(\tilde{k}_\mu)\tilde{\mathbf{g}}_\mu = \tilde{k}_\mu^2\tilde{\mathbf{g}}_\mu, \quad (17)$$

where \mathbf{D} is defined by Eq. (6) but is a function of eigenvalue \tilde{k}_μ .

The solution of the frequency-independent EVP requires

$$\det(\mathbf{D}(\tilde{k}_\mu) - \tilde{k}_\mu^2\mathbf{I}) = 0. \quad (18)$$

As Eq. (8) includes the inverse of $(\mathbf{D} - k^2\mathbf{I})$, it suggests that eigenvalues of Eq. (17) are exactly the poles of $s_{n,n',p,p'}$ (and, in general, the scattering matrix). In general, \tilde{k}_μ takes complex value, and is known as the complex resonance frequency of the scatterer, with $Re(\tilde{k}_\mu)$ being the resonance frequency and $Im(\tilde{k}_\mu)$ characterizing the decay of the mode. For some special cases, \tilde{k}_μ takes a real value, corresponding to localized mode with no radiation loss, which is usually referred to as a trapped mode or bound state in the continuum [10, 19, 11].

As defined, the frequency-dependent EVP yields the bi-orthogonal eigenmodes for the forced response of the scatterer, whilst the frequency-independent EVP produces the modal characteristics of the free vibration of the system. As the response of the scatterer to an incident wave is a forced vibration problem, the use of the frequency-dependent eigenmodes is appropriate.

However, in some previous research, frequency-independent eigenmodes

were sometimes adopted to deal with the forced response of the system [12, 20, 21, 16]. Owing to the nonlinearity of Eq. (17), and hence the absence of orthogonality and completeness of $\{\tilde{\mathbf{g}}_\mu\}$ as a complete set, the modal expansion of the sound field by the frequency-independent bases $\{\tilde{\mathbf{g}}_\mu\}$ lacks justification.

A typical issue encountered when the frequency-independent eigenmodes are used for a forced response problem can be found in Ref. [16], where some peaks/dips in transmission loss (TL) at continuous right-angled corners were attributed to even/odd distributed frequency-independent eigenmodes. An analysis following the procedures in the present paper, however, shows that the extrema in the TL are, as expected, the result of constructive/destructive interference of frequency-dependent eigenmodes, rather than the product of single eigenmodes. Examples of this issue can also be found in the modelling of sound propagation in street canyons using non-orthogonal frequency-independent eigenmodes [20] and in the expansion of the sound field in and outside a parallel sound barrier by frequency-independent eigenmodes [21].

However, the frequency-independent eigensolutions may be used for the forced response of the scatterer in some special cases when (quasi-) trapped modes are involved. Hein *et. al.*, [12], employed a finite element solver to tackle complex resonance for the investigation of quasi-trapped modes and corresponding Fano-resonance in duct-cavity system. It is reasonable to do so because within the narrow band of quasi-trapped modes, Eq. (15) can be further approximated to (readers may refer to the discussion in Sec. 3.2)

$$T_{0,0} \approx \frac{c_2}{\mathcal{K}_\mu^2 - k^2} + c_1 \approx \frac{c_2}{\tilde{k}_\mu^2 - k^2} + c_1, \quad (19)$$

by noting the fact from Fig. 8 that frequency-dependent eigenvalue K_μ can be well approximated by frequency-independent eigenvalue \tilde{k}_μ . Hence, Eq. (19) suggests that \tilde{k}_μ , the frequency-independent eigensolution is able to characterize the frequency dependency of scattering coefficient in such a special case.

5. Conclusions

In this paper, the scattering coefficients of open cavities in an acoustical waveguide were investigated via analysis of eigenmodes. By utilizing the bi-orthogonal frequency-dependent eigenmodes, the scattering coefficients

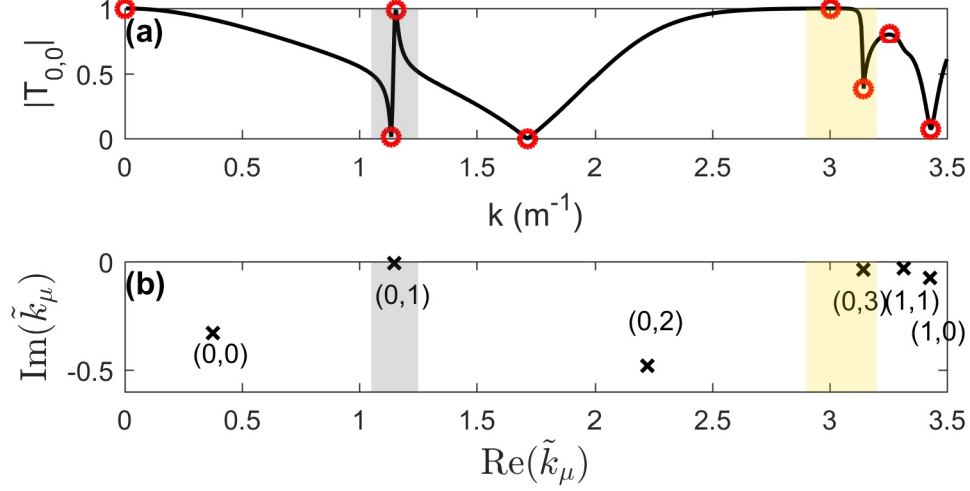


Figure 8: The force response of the asymmetric short cavity considered in Sec. 3.2: (a) amplitude of $T_{0,0}$ and (b) the frequency-independent eigenvalues \tilde{k}_μ of the open cavity.

can be explicitly expressed as the superposition of eigenmodes, allowing for a study of the roles that eigenmodes play in acoustic scattering.

It was shown that the local extrema in the scattering coefficients generally result from the constructive and destructive interference of the resonance and non-resonance modes. In particular, an approximation equation was derived to describe the sharp asymmetric line-shape of scattering coefficients within the narrow-band of Fano resonance induced by quasi-trapped modes. The equivalence of the approximation equation and the standard Fano formula was demonstrated. In addition, it was demonstrated that, in some special cases, the sound scattering coefficient is dominated by single modes, giving rise to resonance transmission

The theoretical analysis was limited to two-dimensional acoustic resonators, and the numerical study was restricted to resonators with simple rectangular cavities. However, it is straightforward to extend the analysis to three-dimensional irregular resonators, where more complicated phenomena may be encountered in the analysis of the frequency-dependent features of scattering coefficients.

Acknowledgements

The financial support from the Australian Research Council (ARC LP) is gratefully acknowledged. The first author is also grateful for the sponsorship from the China Scholarship Council.

Appendix A. Bi-orthogonal relation in Eq. (10)

Let λ_μ and \mathbf{V}_μ be the eigenvalue and eigenvector, respectively, of the non-Hermitian matrix $\mathbf{\Gamma}$ such that

$$\mathbf{\Gamma}\mathbf{V}_\mu = \lambda_\mu \mathbf{V}_\mu, \quad (\text{A.1})$$

where subscript μ is for labelling and λ_μ generally take a complex value.

Similarly, let ζ_μ and \mathbf{W}_μ be the eigenvalue and eigenvector of the adjoint matrix of $\mathbf{\Gamma}$, *i.e.*,

$$\mathbf{\Gamma}^\dagger \mathbf{W}_\mu = \zeta_\mu \mathbf{W}_\mu, \quad (\text{A.2})$$

where $\mathbf{\Gamma}^\dagger \neq \mathbf{\Gamma}$ since $\mathbf{\Gamma}$ is non-Hermitian.

Taking the adjoint of Eq. (A.2) yields:

$$\mathbf{W}_\mu^\dagger \mathbf{\Gamma} = \overline{\zeta_\mu} \mathbf{W}_\mu^\dagger. \quad (\text{A.3})$$

By comparing Eq. (A.1) and Eq. (A.3), one can derive the following correspondence from the uniqueness of the eigenspectrum of $\mathbf{\Gamma}$:

$$\lambda_\mu = \overline{\zeta_\mu}, \text{ all } \mu, \quad (\text{A.4})$$

Right multiplying $\mathbf{V}_{\mu'}$ to the above equation and left multiplying \mathbf{W}_μ^\dagger to Eq. (A.1) (where μ is replaced by μ') and subtracting the resulting equations gives,

$$0 = (\lambda_{\mu'} - \overline{\zeta_\mu}) \mathbf{W}_\mu^\dagger \mathbf{V}_{\mu'}, \quad (\text{A.5})$$

such that the case $\lambda_{\mu'} \neq \overline{\zeta_\mu}$ holds unless $\mathbf{W}_\mu^\dagger \mathbf{V}_{\mu'} = 0$, *i.e.*:

$$\mathbf{W}_\mu^\dagger \mathbf{V}_{\mu'} = \delta_{\mu',\mu} \mathbf{W}_\mu^\dagger \mathbf{V}_{\mu'}. \quad (\text{A.6})$$

With proper normalization, Eq. (A.6) gives the normalized bi-orthogonal relation

$$\mathbf{W}_\mu^\dagger \mathbf{V}_{\mu'} = \delta_{\mu',\mu}, \quad (\text{A.7})$$

which relates the left and right eigenvectors of a non-Hermitian matrix $\mathbf{\Gamma}$.

Furthermore, if $\mathbf{\Gamma}$ is symmetric, then the transpose of Eq. (A.1) is

$$\mathbf{V}_\mu^T \mathbf{\Gamma} = \lambda_\mu \mathbf{V}_\mu^T. \quad (\text{A.8})$$

A comparison with Eq. (A.2) indicates $\mathbf{W}_\mu^\dagger = \mathbf{V}_\mu^T$ such that the bi-orthogonality by Eq. (A.7) is reduced to:

$$\mathbf{V}_{\mu'}^T \mathbf{V}_\mu = \delta_{\mu',\mu}. \quad (\text{A.9})$$

References

References

- [1] L. Kinsler, Fundamentals of acoustics, Wiley, 2000.
- [2] A. Selamet, Z. Ji, Acoustic attenuation performance of circular expansion chambers with extended inlet/outlet, *Journal of Sound and Vibration* 223 (2) (1999) 197–212.
- [3] R. Kirby, J. Lawrie, A point collocation approach to modelling large dissipative silencers, *Journal of sound and vibration* 286 (1) (2005) 313–339.
- [4] T. Graf, J. Pan, Determination of the complex acoustic scattering matrix of a right-angled duct, *The Journal of the Acoustical Society of America* 134 (1) (2013) 292–299.
- [5] P. Wang, T. Wu, Impedance-to-scattering matrix method for silencer analysis, in: INTER-NOISE and NOISE-CON Congress and Conference Proceedings, Vol. 248, Institute of Noise Control Engineering, 2014, pp. 453–460.
- [6] L. Flax, L. Dragonette, H. Überall, Theory of elastic resonance excitation by sound scattering, *The Journal of the Acoustical Society of America* 63 (3) (1978) 723–731.
- [7] J. Pan, J. Leader, Y. Tong, Role of quasinormal modes in controlling the sound transmission loss of duct mufflers, in: Noise and Fluctuations (ICNF), 2015 International Conference on, IEEE, 2015, pp. 1–4.
- [8] J. Kergomard, V. Debut, D. Matignon, Resonance modes in a one-dimensional medium with two purely resistive boundaries: Calculation methods, orthogonality, and completeness, *The Journal of the Acoustical Society of America* 119 (3) (2006) 1356–1367.
- [9] D. N. Maksimov, A. F. Sadreev, A. A. Lyapina, A. S. Pilipchuk, Coupled mode theory for acoustic resonators, *Wave Motion* 56 (2015) 52–66.
- [10] A. Lyapina, D. Maksimov, A. Pilipchuk, A. Sadreev, Bound states in the continuum in open acoustic resonators, *Journal of Fluid Mechanics* 780 (2015) 370–387.
- [11] L. Xiong, W. Bi, Y. Aurégan, Fano resonance scatterings in waveguides with impedance boundary conditions, *The Journal of the Acoustical Society of America* 139 (2) (2016) 764–772.

- [12] S. Hein, W. Koch, L. Nannen, Trapped modes and fano resonances in two-dimensional acoustical duct-cavity systems, *Journal of fluid mechanics* 692 (2012) 257–287.
- [13] C. Viviescas, G. Hackenbroich, Field quantization for open optical cavities, *Physical Review A* 67 (1) (2003) 013805.
- [14] J. D. Jackson, *Classical electrodynamics*, Wiley, 1999.
- [15] K. Pichugin, H. Schanz, P. Šeba, Effective coupling for open billiards, *Physical Review E* 64 (5) (2001) 056227.
- [16] W. Yu, X. Wang, R. Wu, J. Yu, Z. Jiang, D. Mao, Wave propagation in a waveguide with continuous right-angled corners: Numerical simulations and experiment measurements, *Applied Acoustics* 104 (2016) 6–15.
- [17] S. Hein, W. Koch, L. Nannen, Fano resonances in acoustics, *Journal of fluid mechanics* 664 (2010) 238–264.
- [18] A. E. Miroshnichenko, S. Flach, Y. S. Kivshar, Fano resonances in nanoscale structures, *Reviews of Modern Physics* 82 (3) (2010) 2257.
- [19] C. Linton, P. McIver, Embedded trapped modes in water waves and acoustics, *Wave motion* 45 (1) (2007) 16–29.
- [20] A. Pelat, S. Félix, V. Pagneux, On the use of leaky modes in open waveguides for the sound propagation modeling in street canyons, *The Journal of the Acoustical Society of America* 126 (6) (2009) 2864–2872.
- [21] C. Yang, J. Pan, L. Cheng, A mechanism study of sound wave-trapping barriers, *The Journal of the Acoustical Society of America* 134 (3) (2013) 1960–1969.